

Experimental and model based analysis of single und multi stage membrane reactors for the oxidation of short-chain hydrocarbons in a pilot scale

C. Hamel^{1,2}, Á.Tóta², F. Klose², E. Tsotsas², A. Seidel-Morgenstern^{1,2}

¹*Max-Planck-Institut für Dynamik komplexer technischer Systeme, D-39106 Magdeburg, Germany*

²*Otto-von-Guericke-Universität, Institut für Verfahrenstechnik, D-39106 Magdeburg, Germany*

Abstract

This contribution intends to provide a deeper insight into various aspects of multi stage dosing concepts based on an experimental and model based analysis. For this aim the oxidative dehydrogenation (ODH) of ethane to ethylene and propane to propylene on a $\text{VO}_x/\text{Al}_2\text{O}_3$ catalyst were considered as model reactions. For the experimental study, a pilot scale set-up has been constructed with a single stage packed bed membrane reactor and a three stage cascade. The inner/outer membrane diameter was 21/35 mm. Asymmetric alumina membranes were investigated. For comparison with a conventional fixed-bed reactor operation was feasible using the co-feed mode. Reduced simple 1D and more detailed 2D models have been used to identify optimal operation parameters and to describe the concentration and temperature profiles, respectively. Based on a preliminary theoretical analysis, a large set of experimental studies was carried out in a temperature range between 520/630°C (ethane) and 350/500°C (propane). The molar $\text{O}_2/\text{C}_n\text{H}_m$ ratio was varied between 0.5 and 8. In the three stage membrane reactor different dosing profiles could be realised, e.g. increasing (10-30-60), uniform (33-33-33) and decreasing (60-30-10) profiles. Due to the separated and distributed feeding of the reactants, the resulting concentration and residence time profiles and the corresponding product spectra are different in membrane reactors compared to fixed-bed reactors. The analysis performed reveals for the investigated operation range a higher ethylene/propylene selectivity and simultaneously a higher conversion in membrane reactors. In case of low oxygen concentrations the selectivity of the desired product ethylene can be increased significantly compared to the conventional fixed-bed reactor.

The developed detailed 2D models allow a good mathematical description of the exothermal reactions taking place in the membrane reactor. The obtained results for the ODH of propane are similar even though the increase of the propylene selectivity is not so distinctive compared to ethylene.

Keywords: Membrane reactors, pilot plant, selectivity enhancement, ethane, propane

1. Introduction

In the field of chemical reaction engineering intensive research is devoted to develop new processes in order to improve selectivity and yields of intermediate products, like for many industrially relevant reactions (e.g. partial oxidations; [Hodnett, 2000, Sheldon and van Santen, 1995]). There is much room for further improvement based on reaction engineering concepts.

It is well known that in reaction networks optimal local reactant concentrations are essential for a high selectivity towards the target product [Levenspiel, 1999]. If undesired series reactions can occur, it is usually advantageous to avoid backmixing. This is one of the main reasons why partial hydrogenations or oxidations are preferentially performed in tubular reactors [Westerterp, et al., 1984]. Typically, all reactants enter such reactors together at the reactor inlet (co-feed mode). Thus, in order to influence the reaction rates along the reactor length, essentially the temperature is the parameter that could be modulated. In classical papers, summarised by [Edgar and Himmelblau, 1988], the installation of adjusted temperature profiles has been suggested in order to maximise selectivities and yields at the reactor outlet. However, practical realisation of a defined temperature modulation is not trivial. Alternative efforts have been devoted to study the application of distributed catalyst activities [Morbidelli, et al., 2001]. This can be realised e.g. by mixing different catalysts or by local catalyst dilution. An attractive option, which is also capable to influence the course of complex reactions in tubular reactors and which will be discussed in this paper, is to abandon the conventional co-feed mode and to install more complex dosing regimes. The concept is based on the fact that there is a possibility to add one or several reactants to the reactor in a distributed manner. There is obviously a large variety of options differing mainly in the positions and amounts at which components are dosed. Deciding whether a certain concept is useful or not, requires a detailed understanding of the dependence of the reaction rates on concentrations. It is well known that in particular the reaction orders with respect to the dosed component are of essential importance [Lu, et al., 1997a, Lu, et al., 1997b, Lu, et al., 1997c]. Besides dosing one or several components at a discrete position into a fixed-bed reactor there also exists the possibility to realise a distributed reactant feeding over the reactor wall. This can be conveniently realised using tubular membranes. The concept of improving product selectivities in parallel-series reactions by feeding one reactant through a membrane tube into the reaction zone was studied e.g. by [Coronas, et al., 1995a, Diakov and Varma, 2004, Hamel, et al., 2003, Kürten, et al., 2004, Lafarga, et al., 1994, Lu, et al., 2000, Seidel-Morgenstern, 2005, Tota, et al., 2004a, Zeng, et al., 1998].

Further, there are interesting activities attempting to use a catalytically active membrane as a contactor where reactants entering from both sides meet and form the products inside the membrane [Capannelli, et al., 1996, Dittmeyer, et al., 2004, Ozdemir, et al., 2006, Saracco, et al., 1999].

Theoretical and laboratory scale studies focusing on the application of various configurations of membrane reactors in order to improve selectivity-conversion relations in complex reaction systems are available. In particular, several industrially relevant partial oxidation reactions were investigated. Relevant studies were

performed, e.g. for the oxidative coupling of methane [Diakov, et al., 2001, Tonkovich, et al., 1996a], for the partial oxidation of ethane [Al-Juaied, et al., 2001, Coronas, et al., 1995b], propane [Liebner, et al., 2003, Ramos, et al., 2000a, Schäfer, et al., 2003, Ziaka, et al., 1993] and for the ODH of butane [Alonso, et al., 2001, Mallada, et al., 2000b, Tellez, et al., 1997].

In most of these works a single tubular membrane was used to distribute one reactant in the inner volume filled with catalyst particles. In this contribution the partial oxidations of ethane to ethylene and propane to propylene as model reactions performed in a pilot scale membrane reactor were investigated in detail. For such reactions improved integral reactor performance can be achieved further by optimised stage wise dosing of one or several reactants [Hamel, et al., 2003, Thomas, 2003]. Adjusted dosing profiles can be realised e.g. by feeding reactants separately through permeable reactor walls, e.g. through tubular membranes. The concept presented below allows to improve significantly the selectivity and yield with respect to intermediate products.

2. Theory

Principle

Figure 1 illustrates schematically the principle of the well established fixed-bed reactor (FBR) in comparison to the packed bed membrane reactor (PBMR) and a membrane reactor cascade (MR3) applied for controlled multi stage dosing of reactants through the reactor wall, respectively. The three stage membrane reactor allows to realise different dosing profiles, e.g. increasing (10-30-60), uniform (33-33-33) and decreasing (60-30-10) profiles, influencing the local concentration and residence time of the reactants.

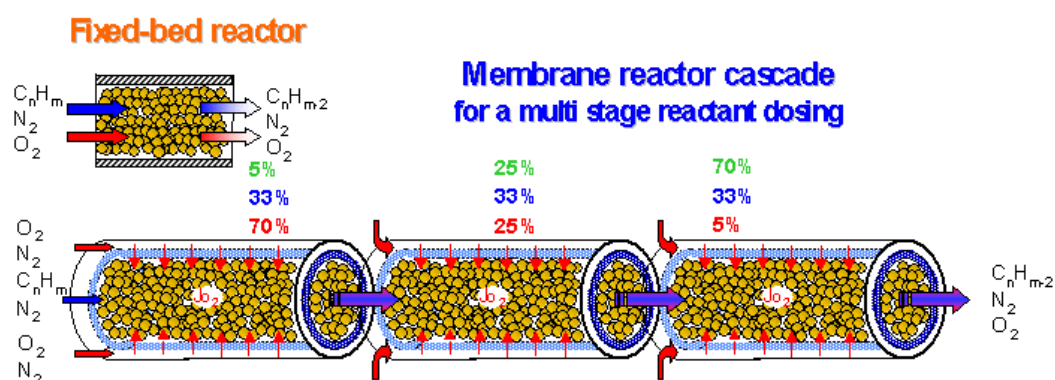


Figure 1: Schematic illustration of reactant feeding in a fixed-bed und in a multi stage membrane reactor cascade

The reactants are fed in the PBMR spatially separated on the inner (tube side, TS) and outer side (shell side, SS) of the membrane. The membrane itself is considered in this contribution to be catalytically inert. The catalyst particles are placed in the tube side of the membrane. The applied dead end reactor configuration allows a feeding of reactants through the membrane in controlled manner, with predefined flow rates. All reactants dosed have to permeate through the membrane. The membrane reactor shown in figure 1 differs from the conventional FBR with respect to residence time behaviour, local concentration, and temperature profiles.

Figure 2a) illustrates typical total flow rates for FBR and PBMR for identical overall feed flow and outlet flow rates without chemical reaction, respectively. For this contribution the total flow rate in the FBR remains constant along the reactor length. All reactants are fed in a co-feed mode at the reactor entrance and have, therefore, the same average residence time in the reactor. For comparison, PBMR profiles are shown for two different ratios of tube side to shell side flow rate ($F_{TS}/F_{SS}=1:8$ and $1:1$). For a uniformly distributed flux through the membrane there is a linear increase in the total flow rate along the reactor length. The slope decreases as the F_{TS}/F_{SS} flow ratio increases. This causes a decreasing residence time of the reactants at the entrance of the reactor. Reactants fed via the shell side have a different residence time distribution. Due to the fact that reactants entering the reaction zone next to the inlet pass a longer reactor distance than molecules entering close to the outlet, the average residence time of the reactants dosed in a PBMR through the membrane is lower compared to a FBR [Tonkovich, et al., 1996b]. Additionally to a one stage membrane reactor a multi stage cascade allows a feeding of different amounts in each stage. Just like the residence time behaviour, the local concentration of the reactants influences the reactor performance significantly. The local concentration has an influence on local reaction rates as well as on conversion and selectivity. Demonstrating the differences between reactor concepts figure 2b) reveals the internal oxygen concentration profiles. Hereby the total amount of oxygen dosed over the membrane in the PBMR is the same as for the FBR. Without a chemical reaction in the FBR the molar fraction of oxygen is constant along the reactor length. Considering the ODH of short-chain hydrocarbons a high oxygen level is undesirable, because it favours the consecutive reactions [Hamel, et al., 2003, Klose, et al., 2003, Tota, et al., 2004b]. Via distributed feeding, the local oxygen concentration can be reduced in a membrane reactor as shown in figure 2b). At low F_{TS}/F_{SS} ratios (i.e. for high trans membrane fluxes) the concentration of oxygen increases rapidly at the entrance. The local, and hence also the averaged oxygen concentration is always lower than in the FBR. It is worthwhile to note that under these flow conditions the local residence time of the hydrocarbons is relatively high near the PBMR inlet. This behaviour can, together with the rapidly increasing oxygen concentration, significantly influence the temperature behaviour of the reactor.

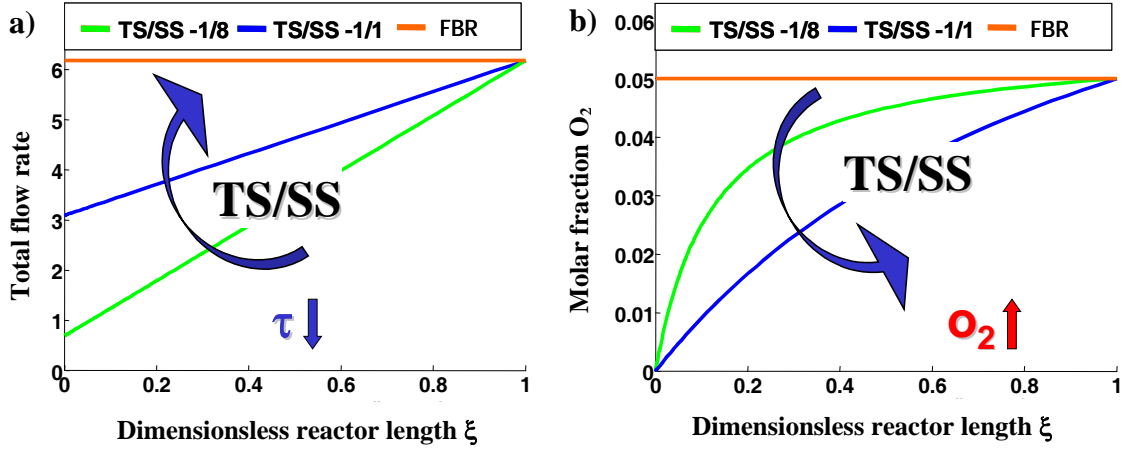


Figure 2: a) Total flow rates and b) molar fraction of oxygen vs. dimensionless reactor length in a fixed-bed and membrane reactor for an identical outlet flow rate

Modelling of membrane reactors

For the simulation of the experimentally investigated membrane and fixed-bed reactors a detailed two dimensional, pseudo homogeneous reactor model was developed and implemented in the simulation tool COMSOL[®]. Under the following assumptions mass and heat balances can be formulated: steady state, ideal gas behaviour, no heat and mass transfer limitations between bulk phase and catalyst particle, as well as inside the catalyst pellets.

Component mass balance:

$$0 = \frac{1}{r} \cdot \frac{\partial}{\partial r} \left[D_{i,r}(r) \cdot r \cdot \frac{\partial c_i}{\partial r} \right] + D_{i,z}(r) \cdot \frac{\partial^2 c_i}{\partial z^2} - \frac{\partial (u_z \cdot c_i)}{\partial z} - \frac{1}{r} \cdot \frac{\partial (r \cdot u_r \cdot c_i)}{\partial r} + (1 - \varepsilon) \cdot \rho_{\text{bulk}} \cdot \sum_j v_{ij} \cdot r_j \quad (1)$$

$$\text{BC: } c_i(z=0) = c_i^{\text{in}}, \frac{\partial c_i}{\partial z}(z=Z) = 0; \frac{\partial c_i}{\partial r}(r=0) = 0; J_i = -D_r \cdot \frac{\partial c_i}{\partial r}(r=R)$$

Where D_r/ D_z is the radial/ axial mass dispersion coefficient [Tsotsas, 1997], c_i is the concentration of component i , u_r/ u_z is the radial/ axial direction of the velocity vector, ε is the porosity of the catalyst bed, v_{ij} is the stoichiometric coefficient of component i for reaction j and r_j is the reaction rate for reaction j .

Heat balance:

$$0 = -\frac{1}{r} \frac{\partial}{\partial r} \left[\lambda_r(r) \cdot r \cdot \frac{\partial T}{\partial r} \right] + \lambda_z(r) \frac{\partial^2 T}{\partial z^2} - c_{\text{pf}} \cdot \frac{\partial (\rho_f u_z T)}{\partial z} - c_{\text{pf}} \cdot \frac{1}{r} \left[\frac{\partial (r \rho_f u_r T)}{\partial r} \right] + (1 - \varepsilon) \cdot \rho_{\text{bulk}} \cdot \sum_j (-\Delta H_{Rj}) \cdot r_j \quad (2)$$

$$\text{BC: } T(z=0) = T^{\text{in}}; \frac{\partial T}{\partial z}(z=Z) = 0; \frac{\partial T}{\partial r}(r=0) = 0; \alpha_w - \text{Model: } -\lambda_r \cdot \frac{\partial T}{\partial r}(r=R) = \alpha_w(T(R) - T_w)$$

and $\lambda_r(r) - \text{Model: } T = T_w$

Where λ_r/λ_z is the radial/ axial heat dispersion coefficient, ρ_{pf} is the fluid density, c_p is the specific heat capacity, ΔH_{Rj} is the reaction enthalpy of reaction j and T is the temperature. Important model parameters for a PBMR are the effective radial and axial heat dispersion coefficients, which were calculated according to two different approaches described in [Tsotsas, 2002]. The first approach called α_w -Model presumes heat dispersion with different but radially constant coefficients in both directions. The second one called the $\lambda(r)$ -Model, was firstly suggested by [Kwong and Smith, 1957], was re-addressed by [Cheng and Vortmeyer, 1988] and refined in an extensive comparison with experimental data by [Winterberg and Tsotsas, 2000a, Winterberg, et al., 2000]. The authors stress that especially in reactive flow problems at low Reynolds numbers the assumption of an inhibiting laminar sublayer at the wall is not appropriate. Therefore, the use of a wall heat transfer coefficient, α_w , can only be artificial. The correlations applied for the calculation of the radial/ axial heat dispersion coefficient are given in [Tota, 2007, Winterberg and Tsotsas, 2000b].

Momentum balance:

To calculate the flow field under reactive conditions the extended Navier Stokes equation and the mass continuity equation were solved. In contrast to BC of the FBR holds for the BC of the membrane reactor at the membrane wall ($r=R$):

$$\text{BC: } u_z(r=R) = 0; \quad u_r(r=R) = J_i \cdot \frac{RT}{P}$$

Where u_z/ u_r is the radial/ axial component of the velocity, P is the pressure under standard conditions and J_i is the molar flux of component i through the membrane. The friction force arising due to the flow through the packed bed was calculated according to [Ergun, 1952] by defining the friction coefficient. For low tube-to-particle diameter ratios a significant part of the flow shifts from the core of the bed towards the reactor wall. This so called flow maldistribution is caused by the non-uniform porosity profile of the packed bed. The effect on the local velocity is pronounced especially at low particle Reynolds number [Winterberg and Tsotsas, 2000c]. To describe the experimentally found damped oscillatory behaviour of the radial porosity profiles, the correlation given by [Hunt and Tien, 1990] was preferred.

Reduced simple 1D model:

A reduced reactor models was applied for an efficient calculation and evaluation of FBR and PBMR in a broad range of operation conditions [Caro, et al., 2006, Hamel, et al., 2006, Tota, et al., 2004a]. The simplified 1D-Model allows further to analyse a series connection of L equally sized stages of isothermal tubular reactors as illustrated in figure 1. All reactants can be dosed in a discrete manner in each stage k at the inlets ($\dot{n}_i^{k,\text{mix}}$) and/or over the walls (j_i^k). All reactor stages are modelled under the

following conditions: negligible axial and radial dispersion, plug-flow, steady state and isothermal operation. Based on these assumptions, the occurrence of M reactions the mass balance for species i and stages k can be written as:

$$\frac{dn_i^k}{d\xi^k} = A \cdot Z \cdot \rho_{bulk} (1 - \bar{\varepsilon}) \cdot \sum_{j=1}^M v_{i,j} \cdot r_j^k + P \cdot Z \cdot J_i^k \quad (3) \quad i=1,N; j=1,M; k=1,L$$

In the equation above $\xi^k = z^k/Z$ is the dimensionless length coordinate, r_j^k is the rate of reaction j and J_i^k is the diffusive flux of component i over the wall of stage k , n_i is the mole number of component i , A is the cross section area and P is the perimeter of the reactor. The catalyst density is denoted by ρ_{bulk} and $\bar{\varepsilon}$ is the averaged porosity of the catalyst bed. To model the configuration shown in figure 1 the following boundary conditions are used together with eq. 3:

$$BC: \quad \dot{n}_i^1(\xi^1 = 0) = \dot{n}_i^{in} \quad (4) \quad \text{and} \quad \dot{n}_i^k(\xi^k = 0) = \dot{n}_i^{k-1}(\xi^{k-1} = 1) + \dot{n}_i^{k,mix} \quad (5) \quad k=2,L$$

The total amounts of component i introduced at all inlets (mix, $L \geq 2$) and over all walls (diff) are:

$$\dot{n}_{i,tot}^{mix} = \sum_{k=2}^L \dot{n}_i^{k,mix} \quad (6) \quad \text{and} \quad \dot{n}_{i,tot}^{diff} = \sum_{k=1}^L \dot{n}_i^{k,diff} = P \cdot Z \cdot \sum_{k=1}^L J_i^k \quad (7)$$

Comparing with predictions of the reduced approach the two dimensional model was found necessary for a detailed analysis of the pronounced concentration, temperature and velocity fields as shown later.

Reaction networks

The oxidative dehydrogenation of ethane to ethylene and propane to propylene on a $VO_x/\gamma-Al_2O_3$ catalyst, which is one of the more suitable ones, were chosen as model reactions. A detailed analysis of the networks and the five main reactions taking place was recently given by [Klose, et al., 2004b] and [Liebner, 2003], respectively.

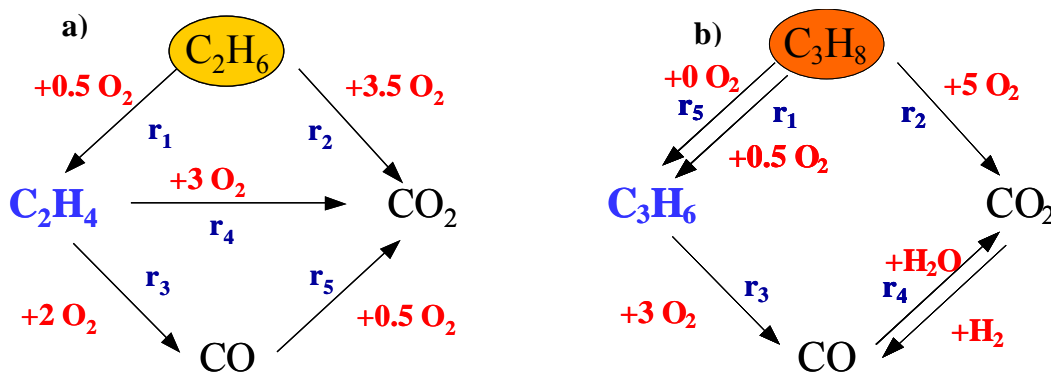


Figure 3: Reaction networks: a) ODH of ethane [Klose, et al., 2004a], b) ODH of propane [Liebner, 2003]

According to the scheme given in figure 3a) ethane is converted in a parallel reaction to CO₂ and to the desired product ethylene. This parallel reaction limits the maximal achievable ethylene selectivity in the reaction to approximately 85%. Additionally the consecutive reaction to CO and the total oxidation can further decrease the olefin selectivity. The authors suggested a kinetic model based on a Mars-van-Krevelen type redox mechanism for the ethylene production and Langmuir-Hinshelwood-Hougen-Watson (LHHW) kinetics for the deep oxidation reactions [Klose, et al., 2004a]. The derived model for the ODH of ethane was found to describe a large set of experimental data from a laboratory scale FBR and PBMR apparatus with good accuracy. In principle the reaction network of propane, given in figure 3b), is similar. Analogue propane is converted in a parallel reaction to CO₂ and to the desired product propylene. Based on the prediction of [Liebner, 2003], propylene can be formed by ODH (r_1) and by thermal dehydrogenation (r_5) in absence of oxygen, respectively. In contrast to the ethane network and considering the lower temperature range the ratio of CO and CO₂ is given by the water gas shift reaction.

Parameter study

In this section the performance of a conventional fixed-bed reactor and a single stage membrane reactor are compared using the oxidative dehydrogenation of ethane for illustration of the reactor behaviour in a broad range of operation conditions. The reaction rates given by [Klose, et al., 2004b] were applied.

As can be seen from figure 4a) the single stage PBMR shows a higher ethylene selectivity than the FBR in the oxygen controlled region for a high contact time corresponding with a high conversion. Increasing the oxygen level leads to a selectivity decrease. Because of unavoidable uncertainties of the kinetic model [Klose, et al., 2004b] the simulation results below an oxygen level of 0.7 vol.% should be evaluated with care. In the conversion plot given in figure 4b) the benefits of the PBMR can be recognised. Conversion differences of up to 15% can be obtained in a broad range of oxygen concentration and residence time. Below 1.5 vol.% oxygen concentration, the FBR shows slightly higher conversions, which can be explained with the higher local oxygen concentration of the FBR. This region is extended towards higher oxygen concentrations with increasing residence time. Differences in the mean residence time of the reactants between FBR and PBMR are still present, but not so significant, as below 250 kgs/m³. With increasing contact time the oxygen level is the only conversion determining factor. The resulting ethylene yields (figure 4c) reveal that there are two preferable regions for the application of a PBMR. The first one is in the residence time controlled region (in this case below approximately 250 kgs/m³). In this region the oxygen concentration can be relatively high. The higher ethylene yields achievable here result from the high reactant conversion. The second region, where simulation postulates the highest PBMR yields, is at longer contact times for oxygen concentrations below 1.5 vol.%.

Finally, a comparison between the dosing concepts will be given by means of a selectivity-conversion plot. To get an insight in the selectivity behaviour of the PBMR for the whole parameter range studied, one can extract all the simulation results for ethylene selectivity and ethane conversion and plot the corresponding values together in one diagram (figure 5). The resulting envelope describes the

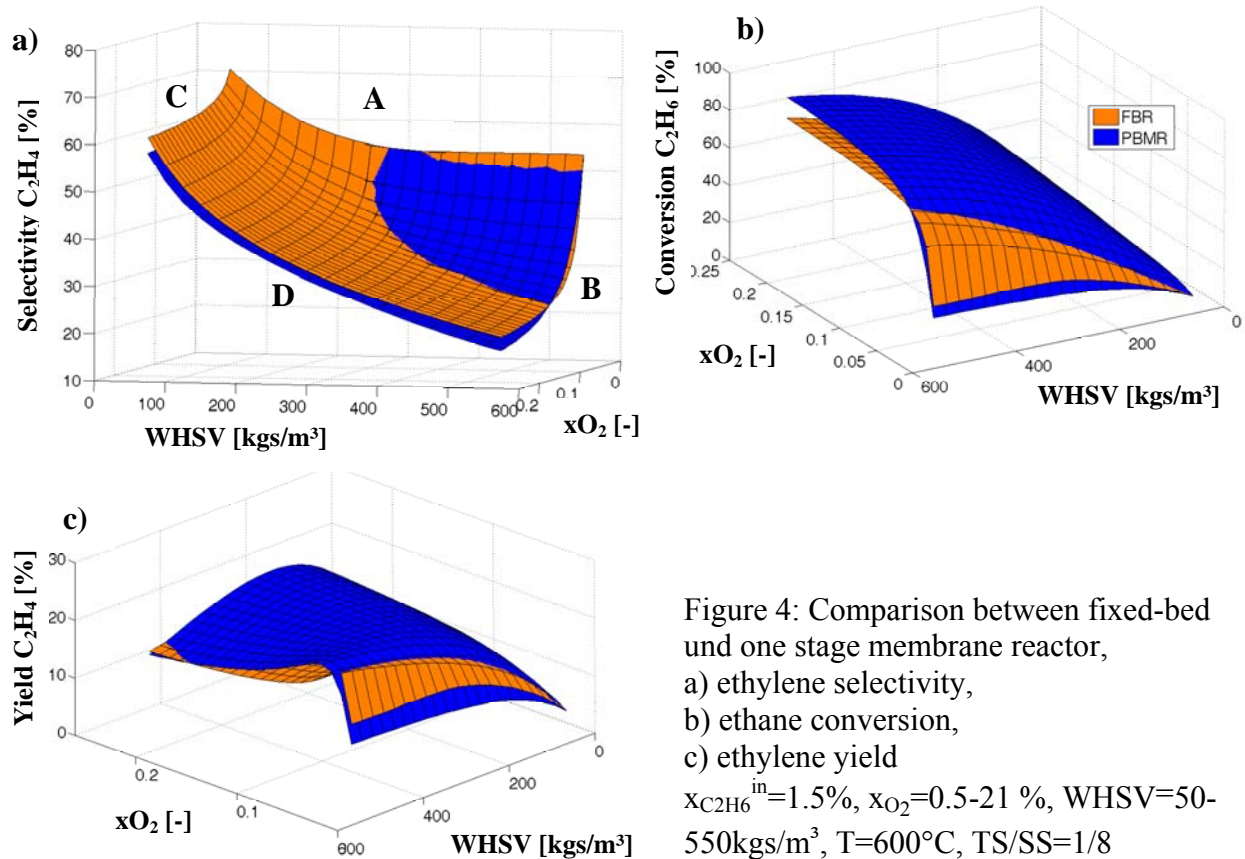


Figure 4: Comparison between fixed-bed and one stage membrane reactor, a) ethylene selectivity, b) ethane conversion, c) ethylene yield $x_{C_2H_6}^{in}=1.5\%$, $x_{O_2}=0.5-21\%$, $WHSV=50-550kgs/m^3$, $T=600^\circ C$, $TS/SS=1/8$

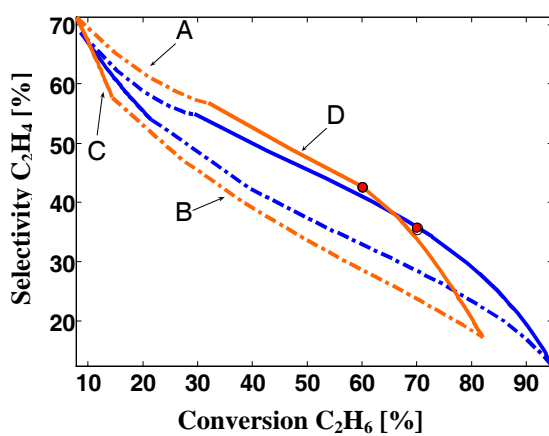


Figure 5: Ethylene selectivity versus ethane conversion in a fixed-bed and one stage membrane reactor $x_{C_2H_6}^{in}=1.5\%$, $x_{O_2}=0.5-21\%$, $WHSV=50-550kgs/m^3$, $T=600^\circ C$, $TS/SS=1/8$

attainable region for the reactor at 600 °C, for the flow rates and reactant concentrations considered. In this special case the borders of the envelope are the edges indicated in figure 4a) as line A,B,C and D. The results given in figure 5 show that for low residence times (line C) and at high oxygen concentration (line D) the PBMR outperforms the FBR. However, in this region the yields are quite low in both reactors. Further, the curves of the PBMR are located inside the operation window of the FBR, thus one can easily find operating parameters where the FBR is superior compared to the PBMR. For ethane per pass conversion below ~ 65 % the FBR allows for higher ethylene selectivity, and therefore higher yields. If higher per pass conversions are needed, the reaction should be carried out in a PBMR, because the ethylene selectivity does not decrease so rapidly than in the FBR. The maximal ethylene yields, marked by white dots, are hardly different in both reactors. According to the simulation result, 25.2 % of the fed ethane is converted to ethylene for the chosen simulation conditions. This was achieved in the membrane reactor for appr. 10 % higher conversion, while the ethylene selectivity was approximately 7 % below that of the FBR.

3. Experimental

Catalyst preparation and membrane structure

The VO_x/γ-Al₂O₃ catalyst used in this study for the ODH of ethane and propane in all reactors was prepared by soaking impregnation of γ-Al₂O₃ with a solution of vanadyl acetylacetonate in acetone followed by a calcination step at 700°C. The vanadium content of the catalyst was 1.4% V. The surface of the calcinated catalyst was 158m²/g, measured by single point BET method with nitrogen as adsorbate. The colour of the fresh catalyst was yellow, indicating vanadium was mainly in the +5 oxidation state. After the measurements, the catalyst colour had changed to a light blue-green. This can be attributed to a significant reduction of V(V) to V(IV), the species responsible for a high ODH selectivity [Zanthoff, et al., 1999]. The tubular ceramic composite membranes in an industrial scale used for feeding air as the oxidant were provided by “Hermsdorfer Institut für Technische Keramik”. These consisted of a mechanically stable α-Al₂O₃ support (average pore diameter: 3µm; thickness: 5.5mm) on which were deposited two more α-Al₂O₃ layers (pore diameters: 1 µm and 60 nm; thickness 25µm) and finally one γ-Al₂O₃ layer (pore diameter: 10 nm; thickness: 2µm). The whole membrane tube had a length of 350 mm, an inner/ outer diameter of 21/ 32mm. Both ends of the membrane were vitrified, leaving in the centre of the membrane a permeable zone of 104 mm (see figure 6b). The mass transport properties of this membrane type were characterised by the authors in a previous study [Hussain, et al., 2006]. During assembling of the membrane reactor, the membrane tube was filled with inert material in the non-permeable zones and with the above described VO_x/γ-Al₂O₃ catalyst in the porous reaction zone.

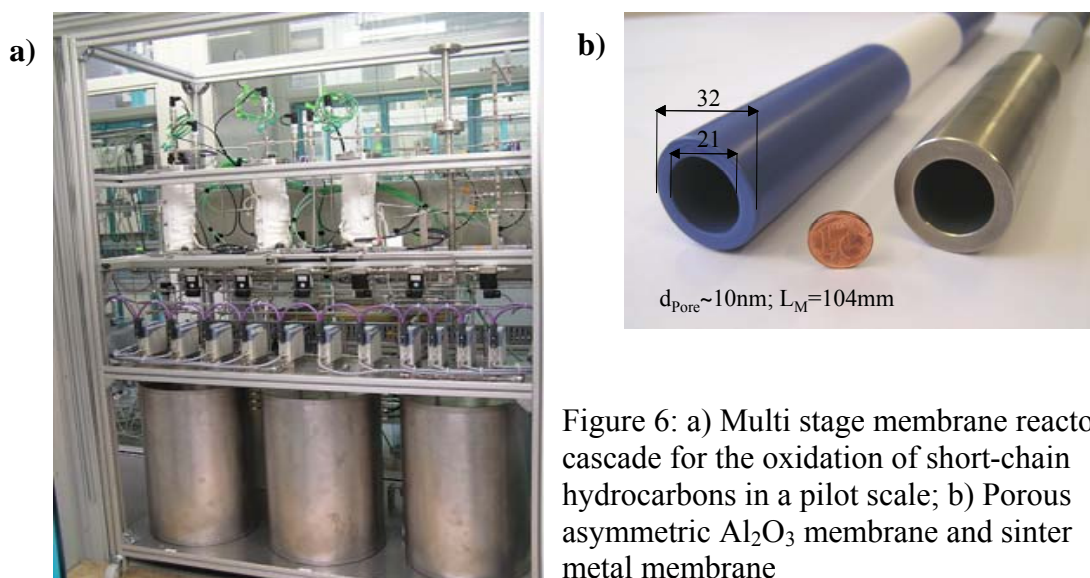


Figure 6: a) Multi stage membrane reactor cascade for the oxidation of short-chain hydrocarbons in a pilot scale; b) Porous asymmetric Al_2O_3 membrane and sinter metal membrane

Set-up

The setup used consists of several units: reactor modules, catalytic afterburner and GC-MSD (Agilent 6890 GC with 5973 MSD) with a 12 port multiposition valve for reactant and product stream analysis (see figure 6a). The reactor modules could be operated alternatively and will be described below. The catalytic afterburner had to prevent hazardous emissions to the laboratory air. A SIMATIC S7 based process control system was implemented to run the unit automatically and recover all process data. Feed mixtures and flow configurations were realised by using electronic mass flow controllers (Bürkert, type 8712). Gas samples were taken from different positions of the reactors as described below by switching the multiposition valve. They transferred via a heated line to the sample valve of the GC-MSD to prevent condensation. All gas samples were analyzed with a GC-TCD/MSD system equipped with a four column configuration with several valves. This configuration included a HP PLOT Q column for the detection of CO_2 , ethane/ propane and ethylene/ propylene, a HP Molsieve 5 A column for the separation of permanent gases and CO, and a FFAP column to detect oxygenates.

Packed bed membrane reactor in a pilot scale

In order to collect experiences in a PBMR with dimensions closed to an industrial scale a pilot-plant was realized with possible feed rates up to 4500 l/h. Beside the possibility to evaluate the development of radial and axial gradients the large scale has the further advantage that the impact of measuring installations, especially thermocouples within the catalyst bed which disturb fluid dynamics, is significantly reduced. The single stage PBMR consists of a stainless steel tube (inner diameter: 38.4 mm) in which the membrane tube filled with the catalyst was inserted. The

reactor was heated by an electric heating sleeve outside the steel tube. Hydrocarbon, for safety reasons diluted 1:10 in nitrogen, was fed on the tube side of the membrane. Air was dosed from the shell side over the membrane into the reactor. The shell side outlet was closed so that all air dosed was pressed via the membrane into the catalyst bed (see figure 1). This configuration is similar to that reported mostly in the recent literature, e.g. as by [Mallada, et al., 2000a, Ramos, et al., 2000b, Tonkovich, et al., 1996b]. However, it differs from that studies, where the shell side outlet was open, so that oxidant transfer over the membrane is influenced by diffusion [Farrusseng, et al., 2001, Kölsch, et al., 2002]. Pressing all air over the membrane has the advantage of an easy control of the amount of air inserted. In this way the membrane was used as a non perm selective oxidant distributor in a dead end configuration. During assembling of the reactor the membrane tube was filled with inert material in the vitrified zones and with the described VOx/ γ -Al₂O₃ catalyst (17 g) in the permeable section (104 mm). Five thermocouples were placed in the center of the tube: at the reactor inlet/outlet, at inlet/ outlet of the porous zone and in the middle of the catalyst bed (see figure 8a). Additionally, thermocouples were installed on the surface of the membrane on the shell and tube side. Gas samples were taken at the tube side inlet and directly after the reactor outlet. The membrane tube was fixed in housing with fixed flanges. Both membrane sides were sealed gas-proof by “Novafit” seals during the assembling of the slip-on flanges at the ends. These flanges had a distance of 125 mm from the hot reaction zone. Because of the material of the seals the head segment temperature was limited to 550°C. It was possible to operate the reactor at catalyst temperatures up to 650°C without any damage of the seals or the membrane itself.

Fixed-bed reactor

For the fixed-bed experiments the same reactor equipment was used as for the PBMR. A complete vitrified asymmetric Al₂O₃ membrane with the same geometry was installed in the membrane reactor. All reactants were fed in a co-feed mode (see figure 1). The application of a vitrified membrane avoids wall reactions compared to a simple fixed-bed reactor made from stainless steel and allows further an investigation under the same heat transfer conditions obtainable using the six thermocouples described above.

Multi stage membrane reactor cascade

The membrane reactor cascade applied for studying the residence time behaviour of the PBMR consists of a series connection of three identical membrane reactors, as described in the previous section. The catalyst masses placed in every PBMR were 17 g. The tube side outlet of each reactor was connected with the tube side inlet of the following reactor using a heated transfer line. The hydrocarbons were inserted in the tube side inlet of the first reactor. Air was introduced from the shell sides of all reactors. To realise different air dosing profiles, e.g. increasing (10-30-60), uniform (33-33-33) and decreasing (60-30-10), the distribution of the air flows between the reactors was changed systematically. Further each reactor could be heated separately by an electrical heating sleeve. However, for the experiments the temperature was

kept equal in all the reactors. Gas sampling was possible at the tube side inlet of the first reactor and at each tube side outlet.

Experimental conditions

Based on the preliminary theoretical analysis shown above, a large set of experimental studies was carried out in a temperature range between 520 - 650 °C (ethane) and 350 - 500 °C (propane). The molar O_2/C_nH_m ratio was varied between 0.5 – 8 and especially near the stoichiometric ratio (hydrocarbon: oxygen=2:1) of the ODH of ethane. The flow rates were relatively low. In our investigations carried out in a pilot scale plant, high space velocities were applied, closer to the requirements set by the industry. The weight hourly space velocity (WHSV) was varied between 100 – 400 kg/m^3 . Additionally, in our study overall oxygen hydrocarbon ratios were below the lower explosion limit, what favours safety of operation. In all PBMR measurements the shell side/tube side feed ratio was adjusted at 8, meaning 88 % of total feed is permeated over the membrane. In these experiments the ratio was kept constant independently on dosed oxygen amount by mixing air with nitrogen for the permeating feed. The reproducibility was checked by conducting product stream analysis more than three times on every set of experimental parameters and additionally by twice repeating every complete run to examine changes of the catalyst itself. The basic reference used to compare the performance of the reactors is the total volumetric flow rate at the reactor outlet under non reactive conditions. Thus, the absolute overall flow rates of the PBMR and of the 3-PBMRC were related to the flow rates of the FBR by considering the ratio of the different catalyst bed volumes.

4. Results and Discussion

Oxidative dehydrogenation of ethane

Comparison between FBR and PBMR

In figure 7 a,c,e) the performance of a single stage PBMR using a ceramic membrane and the conventional FBR in a pilot scale is compared for lean oxygen conditions ($O_2/C_2H_6=1$), and in figure 7 b,d,f) for excess oxygen conditions ($O_2/C_2H_6=5$), respectively. Based on the simulation of the reactor performance presented in part *Parameter study* it can be expected for the PBMR that due to contact time prolongation of ethane inside the catalyst bed ethane conversion is higher in comparison to the FBR as long as oxygen availability becomes not rate determining.

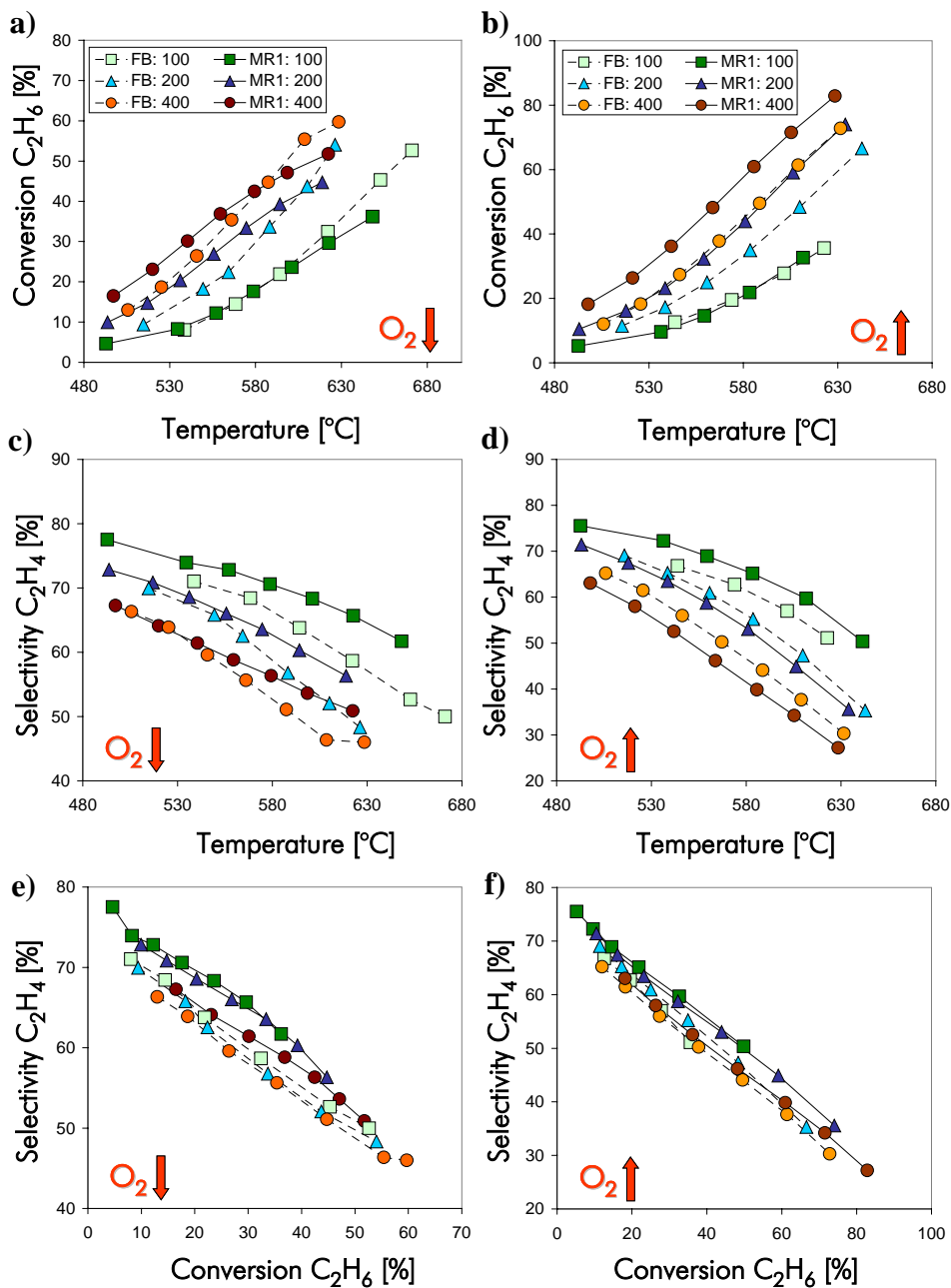


Figure 7: a, b) Conversion ethane vs. temperature c, d) selectivity ethylene vs. temperature, e, f) selectivity ethylene vs. conversion, : temperature, : $x_{C_2H_6}^{in} = 1.5\%$, $O_2/C_2H_6 = 1$ ↓ 0.5 ↑ WHSV = 100-400kgs/m³, catalyst: VO_x/γ-Al₂O₃, (V: 1.4%), BET: 157m²/g, particle diameter: $d_p = 1.0$ mm

However, the parameter study revealed that under oxygen excess conditions the sensitivity of ethylene selectivity to oxygen is low, and for this reason at moderate excess of oxygen the PBMR should provide higher ethylene yields because of the higher level of ethane conversion.

The impact of membrane assisted oxidant dosing in a pilot scale on conversion is given in figure 7a) and 7b) under lean oxygen and for excess oxygen conditions. For an excess of oxygen (figure 7b) and high contact times ($WHSV > 100 \text{ kgs/m}^3$) the PBMR outperforms the FBR significantly. Under conditions of short contact times and for lower temperatures the conversion obtained in the PBMR falls together ($WHSV = 100 \text{ kgs/m}^3$) with that of the corresponding FBR reference experiments independently of the investigated oxygen concentration. The enhanced conversion in the PBMR can be explained by the higher residence time based on the distributed feeding of O_2 and N_2 over the membrane and discussed in part *Principle*. In contrast, under lean oxygen conditions and for temperatures over 600°C the FBR shows a better performance concerning conversion. For these operation parameters the PBMR is limited with respect to oxygen. Thus, the dosed amount of O_2 can not be distributed in the whole provided catalyst. Latter aspect will be investigated in detail in part *Simulations*. Higher conversions of ethane in the FBR can be obtained also for short contact times and for high temperatures. A reason can be found in the different axial temperature profiles which is shown and will be discussed in figure 8.

The selectivity of the desired intermediate product ethylene could be significantly increased in the PBMR especially for lean oxygen conditions but also for conditions of oxygen excess, independently from residence time. Thus, the concept of lowering the local oxygen concentration by a distributed dosing using membranes to avoid series reactions forming CO and CO_2 seems to be successful for the application of ceramic membranes [Hamel, et al., 2003, Thomas, et al., 2001].

Under lean oxygen conditions ethylene selectivity can be significantly enhanced using the PBMR at similar levels of ethane conversion (figure 7e), in contrast under conditions of oxygen excess the selectivity-conversion plots fall together (figure 7f) with those of the corresponding FBR reference experiments. Thus, a benefit regarding ethylene selectivity is given especially at low oxygen to hydrocarbon ratios. Under oxygen excess conditions selectivity-conversion plots of PBMR and FBR are close together.

A further intention to investigate membranes in a pilot scale was to study the axial and radial temperature profiles. Thus, seven thermocouples were placed in the PBMR to measure the temperature at different positions of the catalyst bed and the membrane surface, respectively. The position of the thermocouples illustrated in figure 8a) was already described in part *Packed bed membrane reactor in a pilot scale*. The complex temperature field is given in figure 8b-e). In general it can be recognised: inside the PBMR the inlet temperatures are higher resulting from the heat transfer from shell to tube side especially in the permeable zone of the reactor. For the PBMR the heat transfer is characterised by heat conduction and additionally a high convective radial flow rate based on the distributed feeding of O_2 and N_2 . Thus, the feed of the PBMR can be more rapidly heated up and/or the temperature can be controlled significantly better in comparison to co-feed overall reactant mixture in the FBR where heat transfer is described only by heat conduction.

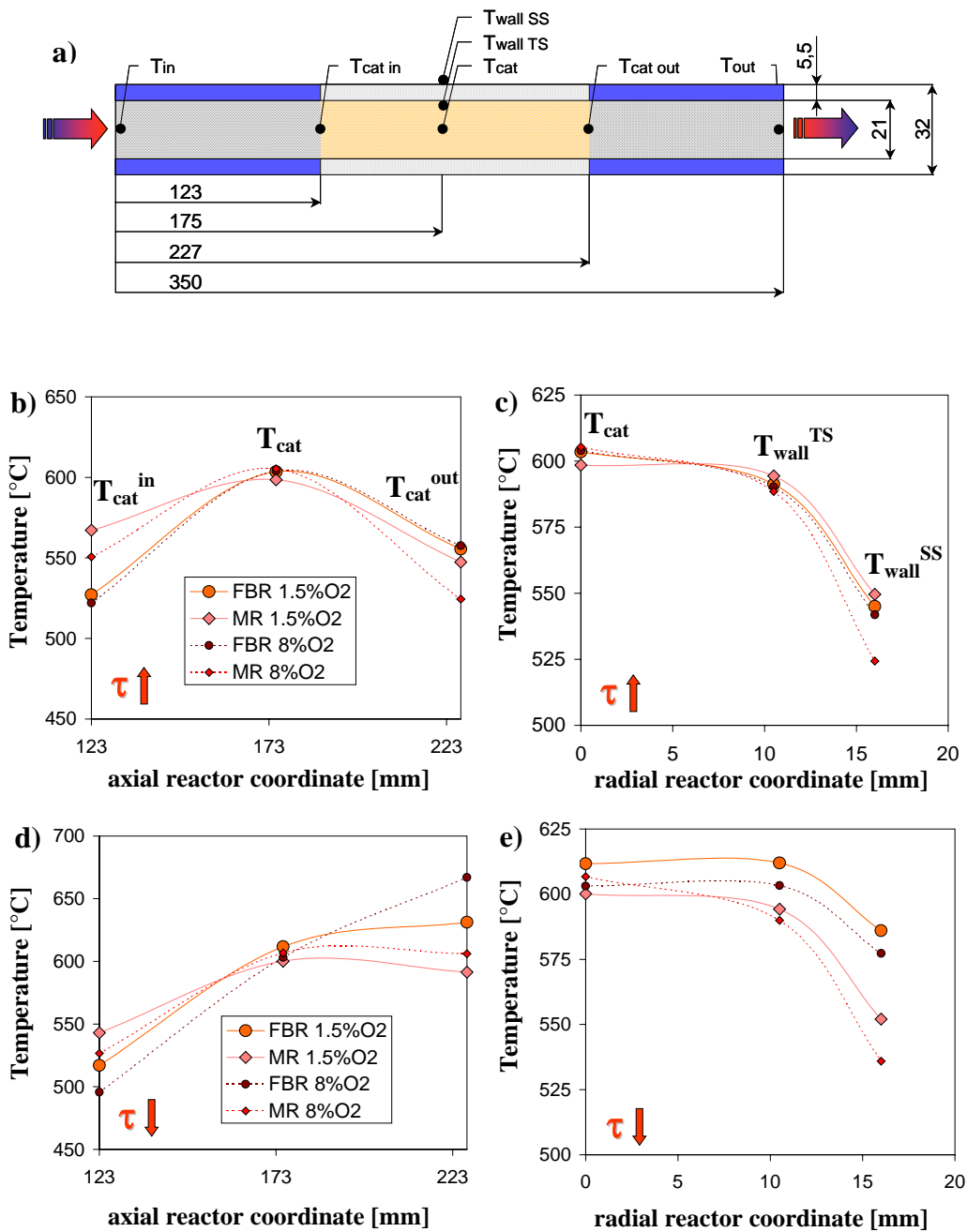


Figure 8: a) Placement of thermocouples, b; d) temperature vs. axial reactor coordinate, c; e) temperature vs. radial reactor coordinate, $x_{C_2H_6}^{in} = 1.5\%$, b; c) WHSV=400kgs/m³ d; e) WHSV=200kgs/m³

As can be seen from figure 8b) for high contact times (WHSV= 400kgs/m³, low feed rates) the differences between PBMR and FBR with respect to temperature is approximately 20 K. For a higher concentration of oxygen (8%) the inlet and outlet

temperatures of the catalyst bed are lower compared to lean oxygen conditions in both reactor concepts. This fact can be explained by the control of the heating coat concerning the temperature in the center of the catalyst bed, T_{cat} . A higher feed concentration of oxygen leads to an increase of the reaction rate and corresponding to an enhanced heat generation. Latter is compensated by the controller which is reducing the heating energy of the coat over the reactor length. A radial temperature distribution can be neglected for the investigated membranes with an inner diameter of 21mm as shown in figure 8c).

In contrast short contact times ($WHSV= 100\text{kg}/\text{m}^3$, see figure 8d) corresponding with high feed flow rates the temperature profiles inside the FBR are much steeper than in the PBMR. In the first one, the temperature in the posterior section of the catalyst bed is near 50 K higher compared to the PBMR. Radial gradients (figure 8e) were developed first at high ethane conversions due to heat accumulation in the central parts of the catalyst bed. However, even at excess oxygen conditions and high feed flow rates they did not exceed 15 K. Thus, in comparison to axial gradients they are only of subordinated importance.

The conversion obtained in FBR and PBMR at different contact time levels is influenced by the established temperature profiles and these are significantly flatter in the PBMR than in the FBR.

Detailed modelling of the pilot scale PBMR

Based on the detailed model presented in part *Modelling of membrane reactors* the concentration, temperature and velocity fields in the PBMR were calculated. As selected results the calculated concentration fields of oxygen and the desired intermediate product ethylene using the $\lambda(r)$ -Model are illustrated in figure 10. The simulated concentration fields of oxygen (fig. 10 a, b) show imposingly the PBMR principle: lowering the local oxygen concentration to avoid series reactions by a membrane assisted distributed dosing. As shown in figure 10 a), under lean oxygen conditions and for temperatures over 600°C the PBMR is limited with respect to oxygen. Thus, the dosed amount of O_2 cannot be distributed and consumed in the whole provided catalyst. Consequently, the FBR reveals under this condition a better performance concerning conversion. On the other hand, for higher concentrations of oxygen (fig. 10b) the catalyst bed is used optimally, but the impact of series reactions increases as can be recognised due to a decreasing ethylene concentration (fig. 10d).

The corresponding temperature profiles obtained with the $\lambda(r)$ -Model and additionally the α_w -Model are depicted in figure 11. The inlet temperature was chosen with respect to the measured inlet temperature of the catalyst bed. Only a marginal hot spot of approximately 10-15K was estimated. However, the $\lambda(r)$ -Model reveals a significant higher and more homogeneous temperature field. Latter corresponds with a higher oxygen concentration close to the wall and a higher conversion of ethane calculated in table 1. The predicted higher oxygen concentration using $\lambda(r)$ -Model was expected, because of the reduced amount of catalyst at the wall, corresponding to the higher local porosity and radial dispersion due to the higher local fluid velocity. Altogether the axial and radial temperature distribution in the PBMR can be sufficiently described using the detailed two dimensional reactor models.

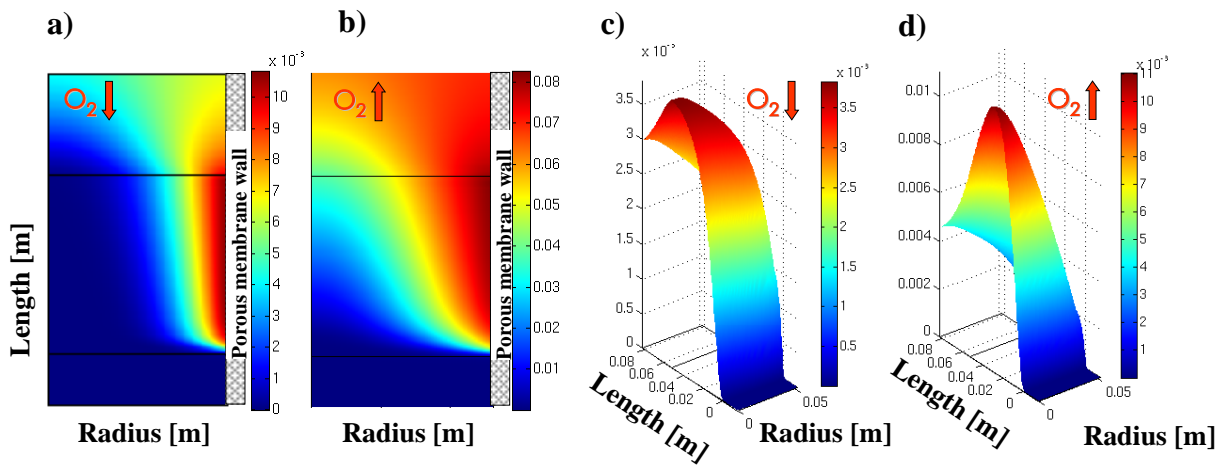


Figure 10: a,b) Calculated concentration fields of oxygen c,d) ethylene concentration using $\lambda(r)$ -Model, $WHSV=400\text{kg}/\text{m}^3$, $C_2H_6^{\text{in}}=1.5\%$, $O_2/C_2H_6=1\downarrow$ and $5\uparrow$, $T=610^\circ\text{C}$

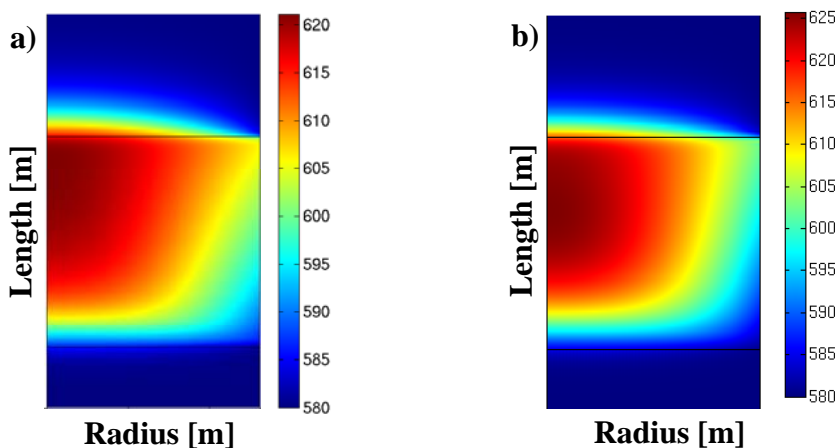


Figure 11: Temperature fields a) α_w -Model b) $\lambda(r)$ -Model, $WHSV=400\text{kg}/\text{m}^3$, $x_{C_2H_6}^{\text{in}}=1.5\%$, $x_{O_2}=1.5\%$, $T^{\text{in}}=580^\circ\text{C}$; $T_{\text{wall}}=610^\circ\text{C}$

An overview with respect to the results of the reduced 1D-Model and the more detailed α_w -Model and $\lambda(r)$ -Model, respectively, in comparison to the experimental data is given in table 1. The oxygen concentrations calculated with the 1D-Model are considerably lower than those of the 2D model, the predicted conversion values (tab. 1) are 3-7 % higher. Hereby, the lower oxygen concentration of the 1D-Model results from higher oxygen consumption. Especially for high contact times ($WHSV=400\text{kg}/\text{m}^3$) ethane conversion as well as ethylene selectivity could be described in a good agreement with the detailed $\lambda(r)$ -Model taking the radial oxygen profile and porosity distribution into account.

Table 1: Evaluation of the used detailed $\alpha_w/\lambda(r)$ -Model and a reduced reactor model by means of the estimated experimental data: $x_{C_2H_6}^{in}=1.5\%$, $x_{O_2}=8\%$, $T=610^\circ C$

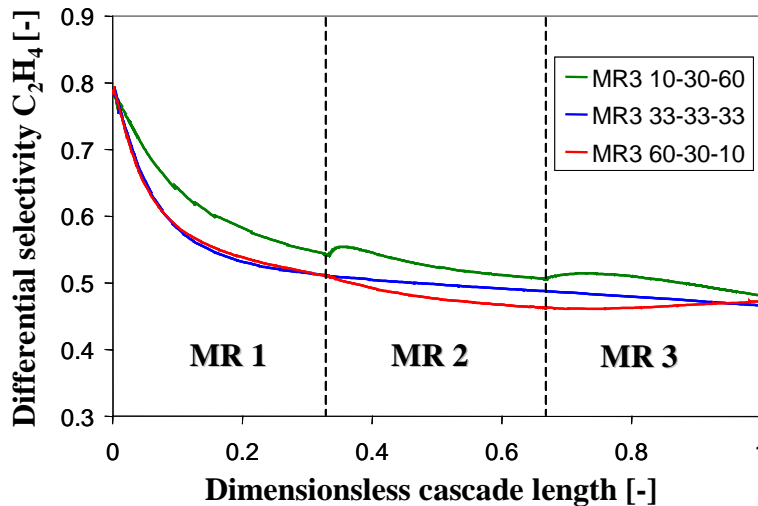
	Experiment		1D-Model		2D- α_w -Model		2D- $\lambda(r)$ -Model	
	[%]		[%]		[%]		[%]	
WHSV [kgs/m ³]	100	400	100	400	100	400	100	400
Conversion C ₂ H ₆	32.6	71.5	35.9	78.8	32.4	65.8	31.7	71.9
Selectivity C ₂ H ₄	59.7	34.2	48.6	30.1	49.7	32.0	51.2	33.4
Yield C ₂ H ₄	19.5	24.5	17.5	23.7	16.1	21.1	16.2	24.1

Results of a three stage membrane reactor cascade – impact of dosing profiles

A detailed proposition concerning the local reaction rates including undesired parallel-series reactions is given by the differential selectivity. For the postulated reaction network of the ODH of ethane to ethylene by [Klose, et al., 2004a] the differential selectivity is defined as follows:

$$S_{diff}^{C_2H_4} = \frac{r_1 - r_3 - r_4}{r_1 + r_2} \quad (7)$$

Especially for the investigation of suitable dosing profiles influencing the local oxygen concentration and contact time in the three stage membrane reactor cascade (MR3) the differential selectivity is a remarkable parameter. In fig. 12 the differential selectivity, calculated by means of the reduced 1D-Model, is illustrated as a function of the dimensionless cascade length. In the MR3 three different dosing profiles could be realised: an increasing (MR3 10-30-60), an uniform (MR3 33-33-33) and a decreasing (MR3 60-30-10) dosing profile as described in detail in part *Experimental*.


 Figure 12: Calculated differential selectivity of ethylene in a three stage membrane reactor cascade, $WHSV=400kgs/m^3$, $x_{C_2H_6}^{in}=1.5\%$, $x_{O_2}=0.75\%$, $T=600^\circ C$

In general the differential selectivity is decreasing over reactor length based on the increasing intermediate concentration of ethylene and the resulting increasing reaction rates r_3 and r_4 , respectively. For the chosen simulation conditions of long contact times and low oxygen concentration (WHSV=400 kgs/m³, x_{O_2} =0.75 %) the increasing dosing profile (MR3 10-30-60) reveals the highest differential selectivity of ethylene. The increasing dosing profile is characterised by a very low oxygen level especially in the first PBMR corresponding with a long contact time. Thus the desired reaction r_1 forming ethylene can take place. Simultaneously, the ethylene consuming following reactions r_3 and r_4 are suppressed due to the low oxygen level. In contrast the uniform (MR3 33-33-33) and a decreasing (MR3 60-30-10) dosing profile are characterised by a higher local oxygen level. The obtained performance parameters of the experimentally investigated three stage membrane reactor cascade are given in figure 13. Based on the kinetics and the reaction network given by [Klose, et al., 2004a] the ethane conversion is increasing and selectivity of the desired intermediate product ethylene is decreasing with increasing temperature as discussed for the single stage membrane reactor PBMR. The highest conversion (fig 13a) can be obtained for the uniform (MR3 33-33-33) and decreasing (MR3 60-30-10) dosing profile. The conversion course as a function of temperature is very similar for both ones. The increasing dosing profile (MR3 10-30-60) reveals a slightly lower conversion behaviour, due to the oxygen limitation especially for high temperatures. In general the membrane reactor cascade demonstrates a better performance with respect to conversion of ethane compared to the single stage PBMR and the conventional fixed-bed reactor (fig. 7). An explanation is the higher residence time of the reactants by means of distributed dosing, which is significant in the cascade anymore. The integral ethylene selectivity of the cascade is illustrated in figure 13b. As predicted in the calculations using the differential selectivity the increasing dosing profile shows the highest ethylene selectivity followed by the constant and decreasing profile. Additionally, the selectivity of ethylene at the outlet of every stage (axial concentration profile) for $T=600^\circ\text{C}$ is given in figure 13c. It can be recognized that at the outlet of the first stage the increasing dosing profile indicates a significant enhancement of the intermediate selectivity. The corresponding lowered local concentration of oxygen is suitable to suppress the following reactions to CO and CO₂, respectively. Due to the condition that the total amount of dosed oxygen at the reactor outlet under non reactive conditions has to be equal, the intensive increase of local O₂-concentration, especially in the third stage, reduces the advance of selectivity at the outlet due to undesired series reactions. Nevertheless, the trend of an enhanced selectivity obtained by the increasing dosing profile can be held up.

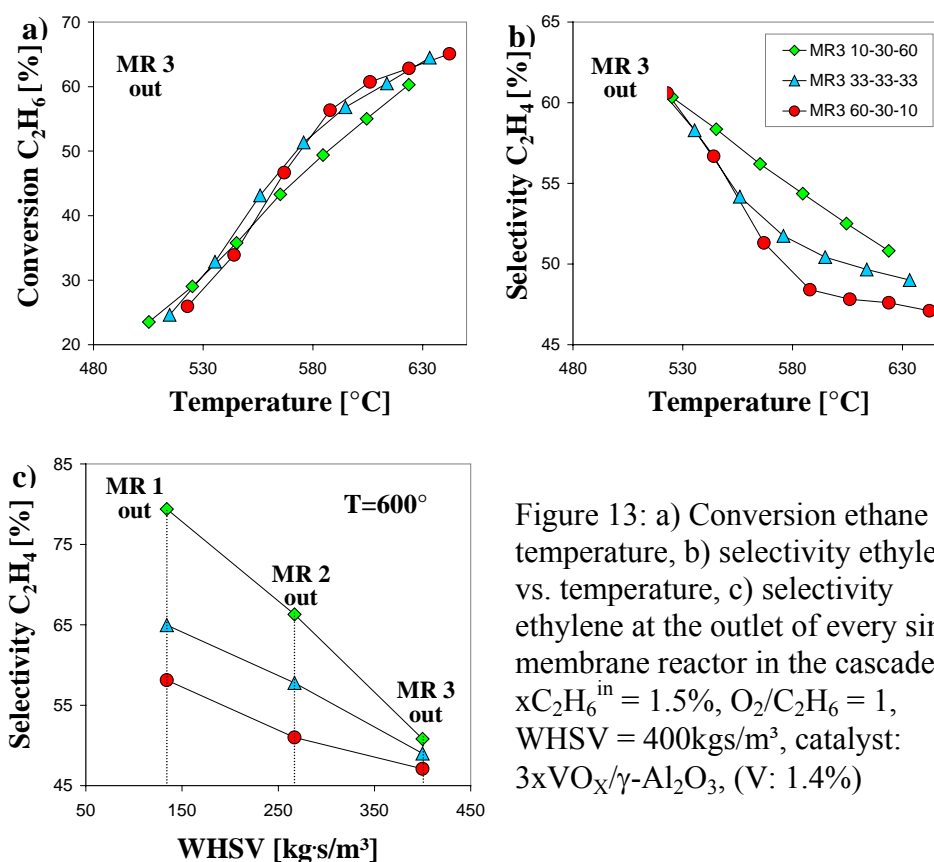


Figure 13: a) Conversion ethane vs. temperature, b) selectivity ethylene vs. temperature, c) selectivity ethylene at the outlet of every single membrane reactor in the cascade: $x_{C_2H_6}^{in} = 1.5\%$, $O_2/C_2H_6 = 1$, $WHSV = 400 \text{ kg/s/m}^3$, catalyst: $3xVO_x/\gamma-Al_2O_3$, (V: 1.4%)

Oxidative dehydrogenation of propane

Comparison between FBR and single stage PBMR

As a second model reaction and from the industrial point of view more interesting reaction the oxidative dehydrogenation of propane to propylene on the same $VO_x/\gamma-Al_2O_3$ catalyst was investigated experimentally. For the propane system a detailed analysis of the reaction network was recently given e.g. by [Liebner, 2003]. In figure 14 a,b the performance of a single stage PBMR using a ceramic membrane and the conventional FBR in a pilot scale is compared for lean oxygen conditions ($O_2/C_3H_8=1$), and in figure 14 c,d for excess oxygen conditions ($O_2/C_3H_8=4$), respectively.

In comparison to the ODH of ethane a similar trend with respect to the selectivity courses can be obtained in figure 14. However, propane selectivity depends stronger on temperature. Thus, the selectivity of propane is decreasing strongly with increasing temperature as well as conversion, nearly independent from the investigated oxygen concentration. Anyhow, under lean oxygen conditions (fig. 14 a,b) and for high contact times, too, a significantly higher selectivity of the desired intermediate

product propane was recognized. This trend is more pronounced for temperatures above 450°C, where the influence of series reactions is more distinctive. Latter can be avoided by a distributed dosing using membranes.

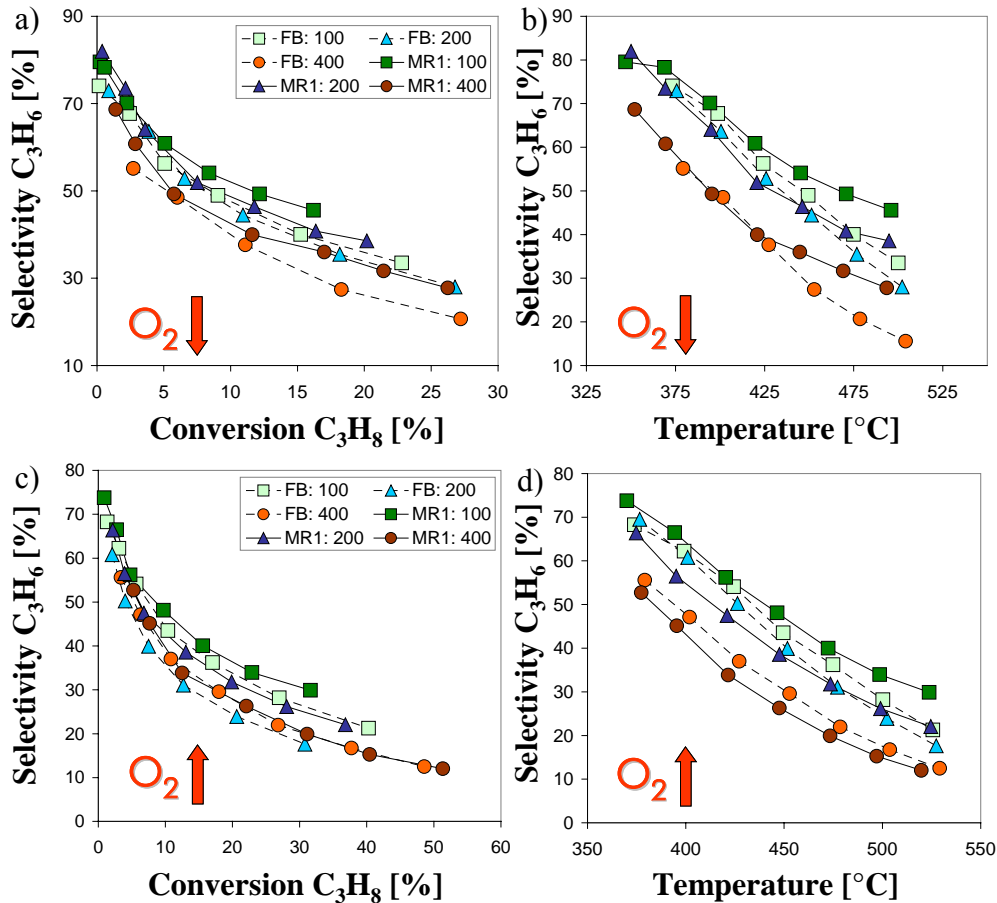


Figure 14: a, c) Selectivity propylene vs. conversion, b, d) selectivity propylene vs. temperature;: $x_{C_3H_8}^{in} = 1\%$, $O_2/C_3H_8 = 1 \downarrow$ a. $4 \uparrow$, WHSV = 100-400kgs/m³,

In contrast to the operation window at lean oxygen conditions the performance of PBMR and FBR is comparable for high contact times (WHSV=400 kgs/m³) and excess conditions concerning oxygen. Under this operating conditions the application of a PBMR is not favourable.

In general the dosing concept via a PBMR is less efficient compared to the ODH of ethane discussed above.

Investigation of the three stage membrane reactor cascade for the ODH of propane

Analogical, selected results of the experimental investigations of the cascade for the ODH of propane are summarised in figure 15. Regarding ethane conversion depicted in figure 15a) the results of all considered dosing profiles are closed together. The dependency with respect to the local oxygen concentration influenced by the dosing

profile is even less pronounced than for the ODH of ethane. Nevertheless, an enhancement of the propane selectivity of approximately 9% can be seen for the increasing dosing profile (MR3 10-30-60) and for higher temperatures (fig. 15b).

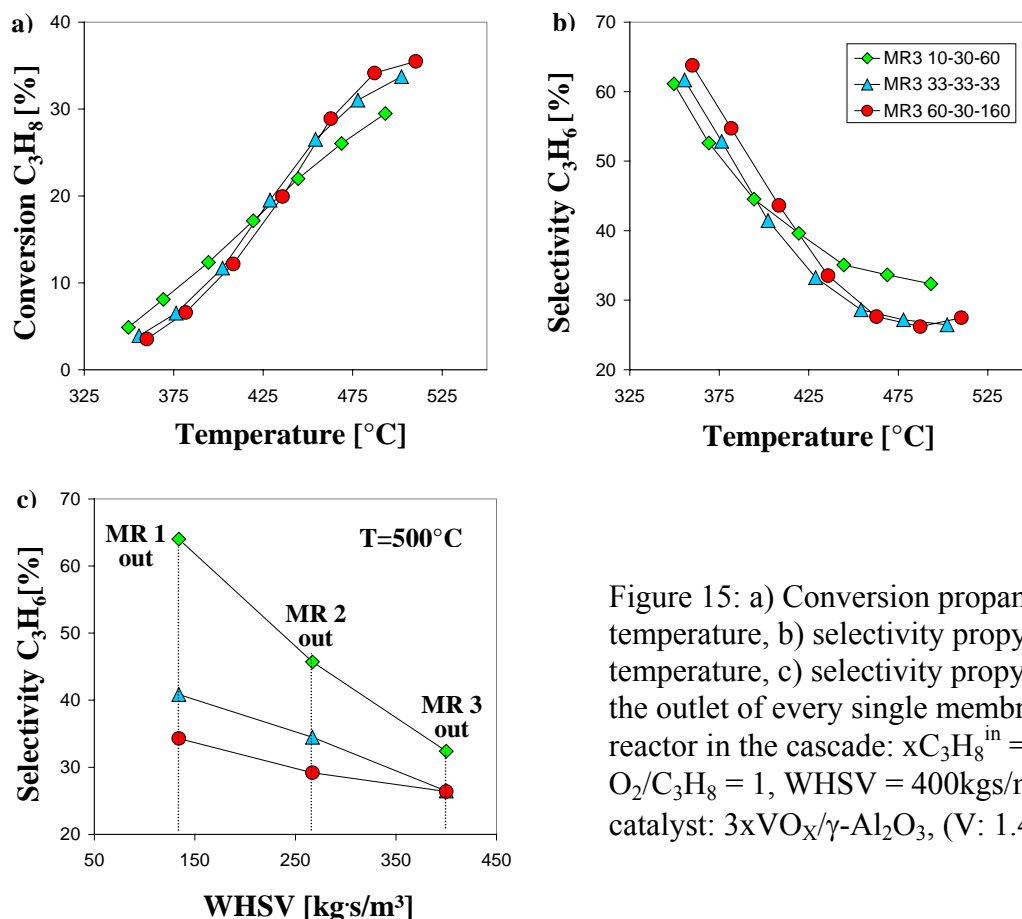


Figure 15: a) Conversion propane vs. temperature, b) selectivity propylene vs. temperature, c) selectivity propylene at the outlet of every single membrane reactor in the cascade: $x_{C_3H_8}^{in} = 1\%$, $O_2/C_3H_8 = 1$, $WHSV = 400 \text{ kg/s/m}^3$, catalyst: $3xVO_x/\gamma-Al_2O_3$, (V: 1.4%)

The illustration of the propane selectivity via the length of the three stage membrane reactor cascade given in figure 15c reveals an advance of the increasing dosing profile along the hole cascade length. Due to the less pronounced sensitivity with respect to oxygen, the intensive increase of local concentration in the third stage does not affect the advance of selectivity caused by undesired series reactions.

5. Summary

Based on an optimal distributed dosing of reactants and the resulting concentration and residence time effects the product spectrum can differ in a membrane reactor compared to a conventional fixed-bed reactor.

The results of the performed theoretical analysis of PBMR and FBR revealed optimal operation conditions for the PBMR, i.e. a maximum ethane conversion and ethylene selectivity, respectively, at higher residence times and a lean oxygen concentration. A

pilot scale packed bed membrane reactor set-up was installed allowing a detailed experimental investigation of single and multi stage membrane as well as conventional fixed-bed reactor operation for the quantified operation conditions.

The experiments using ceramic membranes in a single stage PBMR indicates in case of low oxygen concentrations: selectivity of the desired product ethylene can be increased significantly for simultaneously high ethane conversions compared to the conventional fixed-bed reactor. The application of a multi stage wise dosing by means of an increasing dosing profile recognised a pronounced increase of conversion based on the higher residence time of the reactants for the conditions investigated.

The obtained results for the ODH of propane are similar even though the increase of the propylene selectivity is not so distinctive compared to ethylene. Propylene yield could be further enhanced using a multi stage reactant feeding with an increasing dosing profile.

Three reactor models of different complexity for a mathematical description of the exothermal reactions taking place in the membrane reactor were applied. The oxygen concentrations calculated with the 1D-Model are considerably lower than those of the 2D model result from a higher oxygen consumption. Thus, the predicted conversions overestimate the obtained experimental data. Especially for high contact times ethane conversion as well as ethylene selectivity could be described in a very good agreement with the detailed $\lambda(r)$ -Model taking the radial oxygen profile and porosity distribution into account.

Acknowledgments

The financial support of Deutsche Forschungsgemeinschaft (research group “Membranunterstützte Reaktionsführung, FOR 447/1-1”) is gratefully acknowledged. The authors further thank J. Christel, C. Parzyk, J. Wilke and T. Wolff for their help concerning catalyst preparation and performance of the experiments.

Notation

Latin Letters

A	cross section area [m^2]
c	concentration [vol.%]
c_{pf}	specific heat capacity [$\text{J}/(\text{kg K})$]
D	mass diffusion, dispersion coefficient [m^2/s];
d	diameter [m]
F	volumetric flow rate [m^3/s]
J	molar flux [$\text{mol}/\text{m}^2/\text{s}$]
k	stage number in the cascade
L	total number of stages
M	number of reactions
\dot{n}	molar flux [mol/s]
N	number of components
p	pressure [Pa]
P	perimeter [m]
r	reaction rate [$\text{mol}/(\text{kg s})$]
R	reactor radius; universal gas constant - $8.3145 \text{ J}/(\text{mol K})$
r	radial coordinate
T	temperature [K]
t	time [s]
u	superficial velocity [m/s]
x	molar fraction [%]
z	axial coordinate
Z	total length of the cascade [m]

Greek Letters

α	heat transfer coefficient [$\text{W}/(\text{m}^2 \text{ K})$]
ΔH_R	reaction enthalpy [J/mol]
ε	bed porosity [-]
$\bar{\varepsilon}$	porosity of catalyst bed at infinite distance from the wall [-]

λ	heat conductivity [W/(m K)]
ν	stoichiometric coefficients
ξ	dimensionless length [-]
ρ_f	density [kg/m ³]
ρ_{bulk}	envelop density of the catalyst particle [kg/m ³]
τ	residence time [s]

Sub- and superscripts

<i>diff</i>	feed in a stage over the wall
<i>i</i>	component index; inner
<i>in</i>	inlet
<i>j</i>	reaction index
<i>mix</i>	feed between the stages
<i>p</i>	particle
<i>r</i>	radial direction
<i>s</i>	solid phase
<i>SS</i>	shell side
<i>TS</i>	tube side
<i>w</i>	wall
<i>z</i>	axial direction

Abbreviations

<i>FBR</i>	fixed-bed reactor
<i>MR1</i>	single stage membrane reactor using ceramic membranes
<i>MR1-SM</i>	single stage membrane reactor using sinter metal membranes
<i>MR3</i>	three stage membrane reactor cascade
<i>BC</i>	boundary condition
<i>WHSV</i>	weight hourly space velocity [kg/s/m ³]
<i>TS/SS</i>	tube to shell side ratio
<i>PBMR</i>	packed bed membrane reactor
<i>SM</i>	sinter metal membrane
$S_{diff}^{C_2H_4}$	differential selectivity of ethylene

References

- [Al-Juaied, et al., 2001] M.A. Al-Juaied, D. Lafarga, A. Varma, Ethylene epoxidation in a catalytic packed-bed membrane reactor: experiments and model, *Chemical Engineering Science*, 56, 2, (2001), 395
- [Alonso, et al., 2001] M. Alonso, M.J. Lorences, M.P. Pina, G.S. Patience, Butane partial oxidation in an externally fluidized bed-membrane reactor, *Catalysis Today*, 67, (2001), 151
- [Capannelli, et al., 1996] G. Capannelli, E. Carosini, F. Cavani, O. Monticelli, F. Trifiro, Comparison of the catalytic performance of V₂O₅/ γ -Al₂O₃ in the oxidehydrogenation of propane to propylene in different reactor configurations: 1) Packed-bed reactor, 2) Monolith-like reactor and, 3) Catalytic membrane reactor, *Chemical Engineering Science*, 51, 10, (1996), 1817
- [Caro, et al., 2006] J. Caro, T. Schiestel, S. Werth, H. Wang, A. Kleinert, P. Kölsch, Perovskite hollow fibre membranes in the partial oxidation of methane to synthesis gas in a membrane reactor, *Desalination*, 199, (2006), 415
- [Cheng and Vortmeyer, 1988] P. Cheng, D. Vortmeyer, Transverse Thermal Dispersion and Wall Channeling in a Packed-Bed with Forced Convective Flow, *Chemical Engineering Science*, 43, 9, (1988), 2523
- [Coronas, et al., 1995a] J. Coronas, M. Menendez, J. Santamaria, Use of a ceramic membrane reactor for the oxidative dehydrogenation of ethane to ethylene and higher hydrocarbons, *Industrial & Engineering Chemistry Research*, 34, (1995a), 4229
- [Coronas, et al., 1995b] J. Coronas, M. Menendez, J. Santamaria, Use of a Ceramic Membrane Reactor for the Oxidative Dehydrogenation of Ethane to Ethylene and Higher Hydrocarbons, *Industrial & Engineering Chemistry Research*, 34, 12, (1995b), 4229
- [Diakov, et al., 2001] V. Diakov, D. Lafarga, A. Varma, Methanol oxidative dehydrogenation in a catalytic packed-bed membrane reactor, *Catalysis Today*, 67, 1-3, (2001), 159
- [Diakov and Varma, 2004] V. Diakov, A. Varma, Optimal feed distribution in a packed-bed membrane reactor: the case of methanol oxidative dehydrogenation, *Industrial & Engineering Chemistry Research*, 43, (2004), 309
- [Dittmeyer, et al., 2004] R. Dittmeyer, K. Svajda, M. Reif, A review of catalytic membrane layers for gas/liquid reactions, *Topics in Catalysis*, 29, 1-2, (2004), 3
- [Edgar and Himmelblau, 1988] T.F. Edgar, D.M. Himmelblau, *Optimization of Chemical Processes*, McGraw-Hill, (1988),
- [Ergun, 1952] S. Ergun, Fluid flow through packed columns, *Chem. Eng. Progress*, 35, (1952), 89
- [Farrusseng, et al., 2001] D. Farrusseng, A. Julbe, C. Guizard, Evaluation of porous ceramic membranes as O₂ distributors for the partial oxidation of alkanes in inert membrane reactors, *Separation and Purification Technology*, 25, (2001), 137
- [Hamel, et al., 2006] C. Hamel, A. Seidel-Morgenstern, T. Schiestel, S. Werth, H. Wang, C. Tablet, J. Caro, Experimental and modeling study of the O₂-enrichment by perovskite fibers, *AIChE Journal*, 52, (2006), 3118
- [Hamel, et al., 2003] C. Hamel, S. Thomas, K. Schädlich, A. Seidel-Morgenstern, Theoretical analysis of reactant dosing concepts to perform parallel-series reactions, *Chemical Engineering Science*, 58, (2003), 4483
- [Hodnett, 2000] B.K. Hodnett, *Heterogeneous catalytic oxidation : fundamental and technological aspects of the selective and total oxidation of organic compounds*, John Wiley & Sons, LTD, 2000.
- [Hunt and Tien, 1990] M.L. Hunt, C.L. Tien, Non-Darcian Flow, Heat and Mass-Transfer in Catalytic Packed-Bed Reactors, *Chemical Engineering Science*, 45, 1, (1990), 55
- [Hussain, et al., 2006] A. Hussain, A. Seidel-Morgenstern, E. Tsotsas, Heat and mass transfer in tubular ceramic membranes for membrane reactors, *International Journal of Heat and Mass Transfer*, 49, (2006), 2239
- [Klose, et al., 2004a] F. Klose, M. Joshi, C. Hamel, A. Seidel-Morgenstern, Selective oxidation of ethane over a VOx/ γ -Al₂O₃ catalyst – investigation of the reaction network, *Applied Catalysis A: General*, 260, (2004a), 101

- [Klose, et al., 2004b] F. Klose, M. Joshi, C. Hamel, A. Seidel-Morgenstern, Selective oxidation of ethane over a VOx/gamma-Al₂O₃ catalyst - investigation of the reaction network, *Applied Catalysis a-General*, 260, 1, (2004b), 101
- [Klose, et al., 2003] F. Klose, T. Wolff, S. Thomas, A. Seidel-Morgenstern, Concentration and residence time effects in packed bed membrane reactors, *Catalysis Today*, 82, 1-4, (2003), 25
- [Kölsch, et al., 2002] P. Kölsch, M. Noack, R. Schäfer, G. Georgi, R. Omorjan, J. Caro, Development of a membrane reactor for the partial oxidation of hydrocarbons: direct oxidation of propane to acrolein, *Journal of Membrane Science*, 198, (2002), 119
- [Kürten, et al., 2004] U. Kürten, M. van Sint Annaland, J.A.M. Kuipers, Oxygen distribution in packed-bed membrane reactors for partial oxidations: effect of the radial porosity profiles on the product selectivity, *Industrial & Engineering Chemistry Research*, 43, (2004), 4753
- [Kwong and Smith, 1957] S.S. Kwong, J.M. Smith, Radial Heat Transfer in Packed Beds, *Industrial and Engineering Chemistry*, 49, 5, (1957), 894
- [Lafarga, et al., 1994] D. Lafarga, J. Santamaria, M. Menéndez, Methane oxidative coupling using porous ceramic membrane reactors—I. reactor development, *Chemical Engineering Science*, 49, (1994), 2005
- [Levenspiel, 1999] O. Levenspiel, *Chemical Reaction Engineering*, John Wiley & Sons, (1999),
- [Liebner, 2003] C. Liebner, Einführung der Polythermen Temperatur Rampen Methode für die Ermittlung kinetischer Daten, Universität Berlin, (2003),
- [Liebner, et al., 2003] C. Liebner, D. Wolf, M. Baerns, M. Kolkowski, F.J. Keil, A high-speed method for obtaining kinetic data for exothermic or endothermic catalytic reactions under non-isothermal conditions illustrated for the ammonia synthesis, *Applied Catalysis A: General*, 240, (2003), 95
- [Lu, et al., 2000] Y. Lu, A.G. Dixon, W.R. Moser, Y.H. Ma, Oxidative coupling of methane in a modified γ -alumina membrane reactor, *Chemical Engineering Science*, 55, (2000), 4901
- [Lu, et al., 1997a] Y.P. Lu, A.G. Dixon, W.R. Moser, Y.H. Ma, Analysis and optimization of cross-flow reactors for oxidative coupling of methane, *Industrial & Engineering Chemistry Research*, 36, 3, (1997a), 559
- [Lu, et al., 1997b] Y.P. Lu, A.G. Dixon, W.R. Moser, Y.H. Ma, Analysis and optimization of cross-flow reactors with distributed reactant feed and product removal, *Catalysis Today*, 35, 4, (1997b), 443
- [Lu, et al., 1997c] Y.P. Lu, A.G. Dixon, W.R. Moser, Y.H. Ma, Analysis and optimization of cross-flow reactors with staged feed policies - Isothermal operation with parallel series, irreversible reaction systems, *Chemical Engineering Science*, 52, 8, (1997c), 1349
- [Mallada, et al., 2000a] R. Mallada, M. Menéndez, J. Santamaría, Use of membrane reactors for the oxidation of butane to maleic anhydride under high butane concentrations, *Catalysis Today*, 56, (2000a), 191
- [Mallada, et al., 2000b] R. Mallada, M. Pedernera, N. Menendez, J. Santamaria, Synthesis of maleic anhydride in an inert membrane reactor. Effect of reactor configuration, *Industrial & Engineering Chemistry Research*, 39, 3, (2000b), 620
- [Morbideilli, et al., 2001] M. Morbidelli, A. Gavriilidis, A. Varma, *Catalyst Design: Optimal Distribution of Catalyst in Pellets, Reactors and Membranes*, Cambridge University Press, Cambridge, (2001),
- [Ozdemir, et al., 2006] S.S. Ozdemir, M.G. Buonomenna, E. Drioli, Catalytic polymeric membranes: Preparation and application, *Applied Catalysis a-General*, 307, 2, (2006), 167
- [Ramos, et al., 2000a] R. Ramos, M. Menendez, J. Santamaria, Oxidative dehydrogenation of propane in an inert membrane reactor, *Catalysis Today*, 56, 1-3, (2000a), 239
- [Ramos, et al., 2000b] R. Ramos, M. Menéndez, J. Santamaría, Oxidative dehydrogenation of propane in an inert membrane reactor, *Catalysis Today*, 56, (2000b), 239
- [Saracco, et al., 1999] G. Saracco, H.W.J.P. Neomagus, G.F. Versteeg, W.P.M. van Swaaij, High-temperature membrane reactors: potential and problems, *Chemical Engineering Science*, 54, 13-14, (1999), 1997
- [Schäfer, et al., 2003] R. Schäfer, M. Noack, P. Kölsch, M. Stohr, J. Caro, Comparison of different catalysts in the membrane-supported dehydrogenation of propane, *Catalysis Today*, 82, 1-4, (2003), 15

- [Seidel-Morgenstern, 2005] A. Seidel-Morgenstern, *Integrated Chemical Processes*, Wiley-VCH, 2005.
- [Sheldon and van Santen, 1995] R.A. Sheldon, R.A. van Santen, *Catalytic Oxidation*, World Scientific, (1995),
- [Tellez, et al., 1997] C. Tellez, M. Menendez, J. Santamaria, Oxidative dehydrogenation of butane using membrane reactors, *Aiche Journal*, 43, 3, (1997), 777
- [Thomas, 2003] S. Thomas, *Kontrollierte Eduktzufuhr in Membranreaktoren zur Optimierung der Ausbeute gewünschter Produkte in Parallel- und Folgereaktionen*, Dissertation, (2003),
- [Thomas, et al., 2001] S. Thomas, F. Klose, A. Seidel-Morgenstern, in, 2001.
- [Tonkovich, et al., 1996a] A.L.Y. Tonkovich, D.M. Jimenez, J.L. Zilka, G.L. Roberts, Inorganic membrane reactors for the oxidative coupling of methane, *Chemical Engineering Science*, 51, 11, (1996a), 3051
- [Tonkovich, et al., 1996b] A.L.Y. Tonkovich, J.L. Zilka, D.M. Jimenez, G.L. Roberts, J.L. Cox, Experimental investigations of inorganic membrane reactors: A distributed feed approach for partial oxidation reactions, *Chemical Engineering Science*, 51, (1996b), 789
- [Tota, et al., 2006] A. Tota, C. Hamel, F. Klose, E. Tsotsas, A. Seidel-Morgenstern, Enhancement of intermediate product selectivity in multi-stage reactors-Potential and Pitfalls, *ISCRE 19, Potsdam, Poster 275*, (2006),
- [Tota, et al., 2004a] A. Tota, C. Hamel, S. Thomas, S. Joshi, F. Klose, A. Seidel-Morgenstern, Theoretical and experimental investigation of concentration and contact time in membrane reactors, *Chemical engineering research & design*, 82, (2004a), 236
- [Tota, et al., 2004b] A. Tota, C. Hamel, E. Tsotsas, A. Seidel-Morgenstern, in, 2004b.
- [Tota, 2007] A. Tota, Hlushkou, D., Tsotsas, E., Seidel-Morgenstern, A., *Packed bed membrane reactors*, Kapitel 5 in: *Process intensification* (Herausgeber: F. Keil), Wiley-VCH, Weinheim, in press, (2007),
- [Tsotsas, 1997] E. Tsotsas, *Wärmeleitung und Dispersion in durchströmten Schüttungen*, VDI-Wärmeatlas, Verein Deutscher Ingenieure, (1997), capter Mh
- [Tsotsas, 2002] E. Tsotsas, in *VDI-Wärmeatlas*, Springer, Berlin, 2002, p. 1366.
- [Westerterp, et al., 1984] K.R. Westerterp, W.P.M. van Swaaij, A.A.C.M. Beenackers, *Chemical Reactor design and operation*, John Wiley & Sons, (1984),
- [Winterberg and Tsotsas, 2000a] M. Winterberg, E. Tsotsas, Correlations for effective heat transport coefficients in beds packed with cylindrical particles, *Chemical Engineering Science*, 55, 23, (2000a), 5937
- [Winterberg and Tsotsas, 2000b] M. Winterberg, E. Tsotsas, Correlations for effective heat transport coefficients in beds packed with cylindrical particles, *Chemical Engineering Science*, 55, (2000b), 5937
- [Winterberg and Tsotsas, 2000c] M. Winterberg, E. Tsotsas, Impact of tube-to-particle-diameter ratio on pressure drop in packed beds, *Aiche Journal*, 46, 5, (2000c), 1084
- [Winterberg, et al., 2000] M. Winterberg, E. Tsotsas, A. Krischke, D. Vortmeyer, A simple and coherent set of coefficients for modelling of heat and mass transport with and without chemical reaction in tubes filled with spheres, *Chemical Engineering Science*, 55, 5, (2000), 967
- [Zanthoff, et al., 1999] H.W. Zanthoff, S.A. Buchholz, A. Pantazidis, C. Mirodatos, *Chem. Eng. Sci.*, 54, (1999), 4397
- [Zeng, et al., 1998] Y. Zeng, Y.S. Lin, S.L. Swartz, Perovskite-type ceramic membrane: synthesis, oxygen permeation and membrane reactor performance for oxidative coupling of methane, *Journal of Membrane Science*, 150, (1998), 87
- [Ziaka, et al., 1993] Z.D. Ziaka, R.G. Minet, T.T. Tsotsis, Propane Dehydrogenation in a Packed-Bed Membrane Reactor, *Aiche Journal*, 39, 3, (1993), 526